


Article

Microphytobenthos in the Hypersaline Water Bodies, the Case of Bay Sivash (Crimea): Is Salinity the Main Determinant of Species Composition?

Nickolai Shadrin, Daria Balycheva and Elena Anufrieva * 

Laboratory of Extreme Ecosystems, A.O. Kovalevsky Institute of Biology of the Southern Seas of RAS, 2 Nakhimov Avenue, RU-299011 Sevastopol, Russia; snickolai@yandex.ru (N.S.); dashik8@gmail.com (D.B.)

* Correspondence: lena_anufrieva@mail.ru; Tel.: +7-8692-54-5550

Abstract: In hypersaline water bodies, the microphytobenthos plays a very important ecosystem role and demonstrates variability along with a salinity change. Due to anthropogenic activity, the sharp salinity increase in Bay Sivash occurred after 2014. To assess the changes in the microalgae community during the bay ecosystem transformation, the study was conducted four times in 2018 and 2019. At every sampling period, the samples were taken in a salinity gradient (from 7 to 10 sites). A total of 40 species of microalgae were identified during all research, including Cyanobacteria (Cyanophyceae, 2 species), Ochrophyta (Bacillariophyceae, 35 species), Haptophyta (Prymnesiophyceae, 2 species), and Miozoa (Dinophyceae, 1 species). According to the calculated similarity indices of Jaccard and Czekanowski–Sørensen–Dice, the species composition significantly differed during sampling periods. A total of 15 species were recorded at salinities of 80–90 psu, and 10 species at higher salinities, which contribute 64% of all species found in this study. The microalgae abundance was two times more in the floating green algae mat than on the bottom. There was no significant correlation between the number of species and salinity in all sampling periods. In November 2018, a significant positive correlation between the number of species in the sample and total suspended solids (TSS) and dissolved organic matter (DOM) was revealed. A significant correlation between the cell length in different species and salinity and DOM concentration was noted. Before the onset of the salinity increase, 61 species of microalgae were found in Eastern Sivash, of which only 12 have now been recorded, 31% of the currently found species. The characteristics of the total microphytobenthos abundance also significantly changed during all studies. Many characteristics have changed in the bay: the concentration of total suspended matter and dissolved organic matter, the temperature regime, composition of zoobenthos and plankton, and oxygen concentration. Due to this, it is unlikely that only the salinity increase caused the microphytobenthos changes in the lagoon.

Keywords: bottom microalgae; lagoon; hypersaline; long-term changes; salinity changes; species composition



Citation: Shadrin, N.; Balycheva, D.; Anufrieva, E. Microphytobenthos in the Hypersaline Water Bodies, the Case of Bay Sivash (Crimea): Is Salinity the Main Determinant of Species Composition? *Water* **2021**, *13*, 1542. <https://doi.org/10.3390/w13111542>

Academic Editor: Kevin B. Strychar

Received: 4 May 2021

Accepted: 29 May 2021

Published: 30 May 2021

Publisher's Note: MDPI stays neutral with regard to jurisdictional claims in published maps and institutional affiliations.



Copyright: © 2021 by the authors. Licensee MDPI, Basel, Switzerland. This article is an open access article distributed under the terms and conditions of the Creative Commons Attribution (CC BY) license (<https://creativecommons.org/licenses/by/4.0/>).

1. Introduction

The term ‘Microphytobenthos’ (also ‘microalgae’ as a synonym in the text) is applied to the diverse associations of oxygenic photosynthetic cyanobacteria and eukaryotic algae thriving in aquatic environments at the bottom and every substrate. The Microphytobenthos is an important component in lagoons, marine lakes, and estuaries [1–3]. It plays a significant role in the total primary production, the biogeochemical processes, the stabilization of sediments, and the food webs [4–8]. Bottom microalgae may contribute up to 99% of the chlorophyll content when compared to phytoplankton in shallow lakes and lagoons [7,9–11]. Due to the wind and tidal activity, bottom microalgae resuspension plays a key role in the phytoplankton dynamics, and their proportions can be high in the phytoplankton abundance of shallow lakes and lagoons [7,12]. With decreasing water depth and increasing salinity, the contribution of microphytobenthos to the primary productivity of

aquatic ecosystems increases, while the contribution of phytoplankton decreases [10,13–16]. In hypersaline shallow water bodies, this contribution to total primary production will be especially high. Hypersaline lakes and lagoons, distributed worldwide, especially in the arid areas, are harsh environments. However, they often demonstrate an intense development of microphytobenthos with a high taxonomic diversity of microalgae [3,15,17–24]. Regarding the influence of salinity on the total species richness of microalgae and their taxonomic composition, there are conflicting data that do not allow us to formulate the general patterns (see references above). The scarcity of generalizations on patterns of benthic microalgae variability on different spatial and temporal scales in a salinity gradient can be partly explained by the high diversity of saline water habitats all over the world. Only the accumulation of data on microalgae distribution in the particular water bodies of different regions can lead to finding the general regularities.

Currently, Bay Sivash (the Crimean Peninsula) is the world's largest hypersaline lagoon with a strong salinity gradient from 30 to 100–120 psu [25–27]. Before 2014, the lagoon was brackish water, and only one study of microphytobenthos was conducted [28]. In 2018–2019, authors studied bottom microalgae composition and abundance along a salinity gradient in the bay. This was the first such study in the lagoon after it became hypersaline. The main goals of the study are (1) to provide new data on bottom microalgae of Bay Sivash in a spatial salinity gradient; (2) to analyze the temporal changes of microalgae composition after a sharp salinity increase in the bay; (3) to prove or disprove the hypothesis that salinity is the main or only driver of microalgae composition changes in a salinity gradient. Achievement of the set tasks will contribute to a better understanding of the patterns of ecosystem transformations under a sharp salinity increase. It would also support the organization of sustainable environmental management in the altered Bay Sivash ecosystem.

2. Materials and Methods

2.1. Study Area

Currently, Bay Sivash is Europe's largest shallow semiclosed lagoon/marine lake (area of 2560 km²), separated from the Sea of Azov by the narrow sand Arabat Spit of 112–116 km long [27,29]. There are only two narrow straits on the north connecting the sea with the lagoon (Figure 1).

The maximum depth does not exceed 2 m, with an average of 0.8–1.0 m. Two bay ecosystem transformations occurred in the last half-century. The lagoon was hypersaline, with an average salinity of about 140 psu, reaching up to >200 psu in the southern part before the North Crimean Canal (1963–1975) was constructed. The functioning of the North Crimean Canal gradually changed the lagoon ecosystem and its drainage area [27,29]. The Canal was supplied by Dnieper River freshwater, which was used for irrigation of agricultural lands, and drainage water from cropland was dumped into the lagoon. As a result of this, the average salinity has gradually decreased to 17.0–22.6 psu in 1989–1997 [29]. A different brackish water ecosystem formed with a new composition of abiotic parameters and biota [29]. In this brackish water state, only one study of microphytobenthos was conducted in the lagoon [28]. In April 2014, The Dnieper water supply was ceased into the North Crimean Canal as well as the freshwater discharge from irrigated lands into the lagoon. The sharp salinity increase (from 22 to 100 psu) began in the bay, with cardinal biotic changes in benthos and plankton [25–27]. Currently, there is a strong salinity gradient from 30 to 100 psu and higher. Floating and bottom mats formed by filamentous green algae *Cladophora siwaschensis* (C.J. Meyer, 1922), having high biomass, occupy large areas in the lagoon, leading sometimes to hypoxic and even anoxic events under them [25,26,29]. These mats developed in Bay Sivash before the North Crimean Canal construction. Bay Sivash is divided into the Western Sivash and Eastern Sivash, connected by the narrow Chongar Strait.

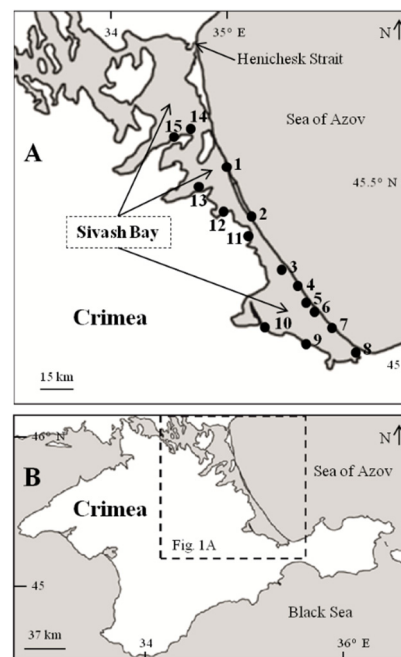


Figure 1. Bay Sivash with sampling stations ((A)—Bay Sivash in Crimea; (B)—Crimea in the Black Sea).

2.2. Sampling and Processing

In different sites of Eastern Sivash, sampling was conducted three times in 2018 (May, June, and November) and in June of 2019 with a parallel evaluation of environmental parameters (Table 1, Figure 1). In total, to analyze the species composition and abundance of bottom microalgae, 39 samples of bottom sediments and 9 of floating green algae mats were taken.

In the mats, samples of 1 to 2 g (wet weight) were taken by tweezers in triplicate. The benthic samples were collected by a benthic tube (diameter 5 cm) in duplicate. Microalgae of bottom sediments were separated by repeated washing with distilled water, followed by sedimentation. Mat samples, washed in distilled water, were dried on filter paper and weighed by a WT-250 electronic balance (Techniprot, Pruszkow, Poland). Microalgae attached to *Cladophora* were removed from filaments by a soft synthetic brush and washed out into a Petri dish with filtered seawater (membrane filter, pore diameter 1 μm). This process was monitored under a microscope. The microalgae were brushed off from filaments, which were washed until a complete absence of microalgae was observed under a microscope using randomly selected fragments of filaments. The final suspension was fixed by 96% alcohol, 2 mL per 100 mL of a sample. Microalgae were analyzed using a light microscope Olympus BX53F (Olympus Corporation, Tokyo, Japan) at magnifications of 10×20 , 10×40 , and 10×100 . Microalgae photography was carried out by a GRYPHAX ARKTUR (JENOPTIK Optical Systems GmbH, Jena, Germany) camera using the GRYPHAX microscope camera software at different magnifications. During all sampling, salinity and temperature were measured by a Kellong WZ212 (Kelilong Electron Co. Ltd., Fuan, China) manual refractometer and a PHH-830 (OMEGA Engineering, INC., Norwalk, CT, USA) electronic thermometer, respectively. In May and November of 2018 as well as in June of 2019, determination of the concentration of total suspended solids (TSS) and dissolved organic matter (DOM) was also conducted by Mr. A. Latushkin using the biophysical complex 'Condor' (produced by Akvastandard-Yug, Sevastopol, Russia) as described in [29]. The authors follow the current classification of Algae according to the AlgaeBase website [30].

Table 1. Characteristics of sampling points in Bay Sivash (2018–2019).

Station	Coordinates	May, 2018			November, 2018			June, 2019		
		S, psu	TSS, mg L ⁻¹	DOM, mg L ⁻¹	S, psu	TSS, mg L ⁻¹	DOM, mg L ⁻¹	S, psu	TSS, mg L ⁻¹	DOM, mg L ⁻¹
1	45°45′37.0″ N 34°57′57.0″ E	–	–	–	–	–	–	70	3.72	3.40
2	45°37′9.0″ N 35°04′40.0″ E	–	–	–	86	6.98	4.45	68	9.80	3.77
3	45°31′13.7″ N 35°11′12.9″ E	76	16.95	4.16	90	1.88	3.76	84	26.66	13.32
4	45°29′04.7″ N 35°13′27.9″ E	77	16.59	3.97	90	1.03	3.44	84	24.55	14.65
5	45°27′19.5″ N 35°13′27.9″ E	77	23.15	3.68	82	4.56	4.36	86	28.46	15.35
6	45°24′43.5″ N 35°17′33.8″ E	77	24.20	3.73	100	6.85	4.35	84	21.11	13.75
7	45°23′04.7″ N 35°19′44.6″ E	77	20.81	4.09	89	6.47	4.31	84	15.95	12.85
8	45°17′14.3″ N 35°28′01.2″ E	82	12.20	3.80	87	12.38	7.98	100	8.69	7.14
9	45°19′05.5″ N 35°14′59.8″ E	75	18.56	4.12	92	70.16	42.14	–	–	–
10	45°21′04.2″ N 35°06′06.5″ E	75	24.76	4.13	90	29.27	21.56	88	14.92	7.36
11	45°37′48.3″ N 35°01′54.8″ E	56	5.64	3.21	63	3.55	3.76	70	14.32	6.46
12	45°40′48.8″ N 34°54′55.2″ E	52	3.50	2.93	56	3.44	3.47	66	7.73	3.41
13	45°44′00.8″ N 34°48′10.3″ E	39	5.53	2.90	42	23.83	11.92	54	4.83	3.36
14	45°52′38.8″ N 34°44′33.3″ E	36	3.11	3.01	38	1.31	2.97	50	2.45	3.56
15	45°52′42.6″ N 34°42′09.0″ E	30	2.37	2.66	30	24.02	11.84	35	9.87	2.98

S—salinity; TSS—total suspended solids; DOM—dissolved organic matter.

The number of microalgae was determined by counting cells using a light microscope in the Goryaev chamber (IBSS, Sevastopol, Russia) (volume of 0.9 mm³), in triplicate. The total number of microalgae on the filaments was calculated:

$$N = n \times V \times S_f^{-1} \times V_k^{-1} \quad (1)$$

where N—the total number of microalgae, cells m⁻²; n—the number of cells in the Goryaev chamber; V—the sample volume, mL; S_f—total filament area in a sample, m²; V_k—Goryaev’s chamber volume equal to 0.0009 mL.

The filament specific surface area (S_f/W)_{Cl} was calculated using the equation obtained by simple transformations, provided that the mass of *Cladophora* is equal to its volume, i.e., specific gravity is 1:

$$(S_f/W)_{Cl} = 4 \times d^{-1} \quad (2)$$

where S_f—total filament area in a sample, m²; W—the wet weight of mat sample, g; d—the average diameter of the *Cladophora* filaments, m, which, as shown earlier, is equal to 2.45 × 10⁻⁵ m [24].

The microalgae biomass was calculated:

$$B = \rho \times b \times V \times S^{-1} \times V_k^{-1} \quad (3)$$

where B —biomass, mg m^{-2} ; ρ —the specific microalgae gravity of $1.2 \times 10^{-9} \text{ mg } \mu\text{m}^{-3}$ for benthic diatoms, or for others, $1 \times 10^{-9} \text{ mg } \mu\text{m}^{-3}$ [31]; b —the total biological volume of cells in the Goryaev chamber, determined by [32], μm^3 ; V —the sample volume, mL; S —total filament area in a sample, m^2 ; V_k —Goryaev's chamber volume, mL.

Microalgae of soft-bottom sediments were separated by repeated washing with distilled water, followed by sedimentation. Then, after washing, the sedimented cells were placed in a measuring cylinder with a known diameter. The quantitative characteristics of microalgae were calculated for the volume of the sedimented cells in the sample using the formula for determining the volume of a cylinder:

$$V_{\text{sed}} = \pi \times r^2 \times h \quad (4)$$

where V_{sed} —the volume of the sediment obtained, cm; r —the radius of the measuring cylinder, cm; h —the height of the sedimented cells in the measuring cylinder, cm.

From this volume, 2 mL was taken three times, and samples were examined to identify the species and determine the quantitative characteristics. The number of cells per unit bottom area was calculated:

$$N = V_{\text{sed}}/S_t \quad (5)$$

where S_t —a benthic tube area equaling 15.9 cm^2 .

2.3. Data Analysis

In the standard program MS Excel 2007, we calculated average values, standard deviations (SD), coefficients of variation (CV), correlation (R), determination (R^2), and parameters of the regression equations. The confidence level (p) of correlation coefficients was calculated [33]. The evaluation of the significance of differences was made by Student's t -test, with performing normality test [34] before this.

The general mat characteristics (biomass and total filaments area per m^2 of the bottom) were calculated according to [24]. To evaluate the similarity of the species composition in the different periods, the Jaccard and Czekanowski–Sørensen–Dice similarity indices were applied [35]:

$$KJ = c/(a + b - c) \quad (6)$$

$$KCSD = 2c/(a + b) \quad (7)$$

where KJ and $KCSD$ —Jaccard and Czekanowski–Sørensen–Dice similarity coefficients, respectively; c —number of species common to both plots or periods; a —number of species found in the first case; b —number of species found in the second case. Threshold values of 0.42 (Jaccard) and 0.59 (Czekanowski–Sørensen–Dice) were used to determine the similarity/dissimilarity of the species composition [35].

3. Results

Abiotic characteristics at sampling stations are given in Table 1. Salinity during the sampling period varied from 30 to 100 psu. In November 2018, there was a strong northeast wind, which affected the spatial distribution of suspended matter. At the leeward coast, the concentration of suspended matter was significantly higher.

A total of 40 species of microalgae were identified during all research, including Cyanobacteria (Cyanophyceae, 2 species), Ochrophyta (Bacillariophyceae, 35 species), Haptophyta (Prymnesiophyceae, 2 species), and Miozoa (Dinophyceae, 1 species) (Table 2). Salinity ranges are also given in (Table 2).

In May–June 2018, a total of 23 species were recorded at the bottom, and 11 species were recorded in floating mats. At the bottom, 13 species were found in November 2018 and 29 species in June 2019. In May–June 2018, microalgae were absent in two bottom samples out of 14 (in 14% of samples), and microalgae were present in all samples of the mats. In November 2018 and June 2019, microalgae were absent in two bottom samples out of 11 taken (in 18%). Those empty samples were excluded from further analysis. In May–

June 2018, the number of species in one bottom sample, where they occurred, varied from 1 to 10 species (average 5.4, CV = 0.48), and in mat samples, the number varied from 4 to 8 (average 6.0, CV = 0.28). There were no differences in the sets of species on the bottom and in the mats; it was just that the list of species encountered in the mats was shorter. The number of species in one bottom sample taken in November 2018 ranged from 1 to 5 (average 2.70, CV = 0.59), and in June 2019 ranged from 3 to 10 (average 6.10, CV = 0.33). There was no significant correlation between the number of species and salinity in all sampling periods.

In November 2018, a significant positive dependence of the number of species in the sample on TSS was revealed ($R = 0.721$, $p = 0.001$):

$$M = 1.083 + 0.838 \text{ Lg (TSS)} \quad (8)$$

where M is the number of species; Lg (TSS) is the logarithm of the concentration of TSS, mg L^{-1} .

A similar reliable dependence of the number of microphytobenthos species on the amount of DOM was found ($R = 0.649$, $p = 0.03$):

$$M = 0.692 + \text{Lg (DOM)} \quad (9)$$

where Lg (DOM) is the logarithm of the DOM concentration, mg L^{-1} .

No correlations were found for the samples collected in June 2018 and 2019.

Table 2. Species composition of microphytobenthos in Bay Sivash (2018–2019).

Species	Salinity Range for a Species, Psu	Frequency of Occurrence, %				Found Before		
		May and June 2018		November 2018	June 2019	The Sea of Azov	Eastern Sivash Before 2014	Crimean Hypersaline Lakes
		Bottom	Mat	Bottom	Bottom			
Ochrophyta								
<i>Achnanthes adnata</i> Bory, 1822	52–92	67	100	78	56	[28]	[28]	[21,24]
<i>Amphitetras antediluviana</i> Ehrenberg, 1840	88–90	0	0	11	11	–	–	–
<i>Amphora macilenta</i> var. <i>maeotica</i> Proshkina-Lavrenko, 1963	87	0	0	11	0	–	–	–
<i>Amphora ovalis</i> (Kützing) Kützing, 1844	100	0	0	0	11	[28]	–	[21]
<i>Amphora</i> sp.	77	17	17	0	0	–	–	–
<i>Ardissonea crystallina</i> (C. Agardh) Grunow, 1880	66–92	0	0	11	11	[28]	[28]	[21,24]
<i>Campylodiscus neofastuosus</i> Ruck and Nakov in Ruck et al., 2016	38–90	8	0	44	22	–	–	[21]
<i>Cocconeis kujalnitzkensis</i> Gusliakov and Gerasimiuk, 1992	52–100	67	100	44	67	–	–	[21]
<i>Cocconeis placentula</i> Ehrenberg, 1838	66–88	0	0	0	22	[28]	–	[24]
<i>Cocconeis scutellum</i> Ehrenberg, 1838	35–70	0	0	0	44	[28]	[28]	[21,24]
<i>Coronia daemeliana</i> (Grunow) Ruck and Guiry, 2016	52–70	8	0	0	11	–	–	–
<i>Diploneis bombus</i> (Ehrenberg) Ehrenberg, 1894	52	8	0	0	0	[28]	–	[21]

Table 2. Cont.

Species	Salinity Range for a Species, Psu	Frequency of Occurrence, %				Found Before		
		May and June 2018		November 2018	June 2019	The Sea of Azov	Eastern Sivash Before 2014	Crimean Hypersaline Lakes
		Bottom	Mat	Bottom	Bottom			
<i>Grammatophora marina</i> (Lyngbye) Kützing, 1844	54–88	8	0	0	22	[28]	[28]	[21]
<i>Gyrosigma balticum</i> (Ehrenberg) Rabenhorst, 1853	35	0	0	0	11	[28]	[28]	–
<i>Gyrosigma fasciola</i> (Ehrenberg) J.W.Griffith and Henfrey, 1856	56	8	0	0	0	–	–	–
<i>Halamphora coffeiformis</i> (C.A. Agardh) Levkov, 2009	52–100	50	67	11	56	[28]	[28]	[21,24]
<i>Lyrella lyroides</i> (Hendey) D.G. Mann, 1990	88	8	0		11	–	–	–
<i>Mastogloia braunii</i> Grunow, 1863	56–84	8	0	11	11	[28]	–	[21,24]
<i>Navicula menisculus</i> Schumann, 1867	52–86	8	33	0	11	[28]	–	[21,24]
<i>Navicula</i> sp. 1	52–100	58	100	0	33	–	–	–
<i>Navicula</i> sp. 2	88	8	0	0	0	–	–	–
<i>Nitzschia hybrida</i> var. <i>hyalina</i> Proschkina-Lavrenko, 1963	52–88	17	17	0	11	[28]	–	[21,24]
<i>Nitzschia sigma</i> (Kützing) W. Smith, 1853	84	0	0	0	11	[28]	[28]	[21,24]
<i>Nitzschia tenuirostris</i> Mereschkowsky, 1902	54–77	8	33	0	22	[28]	–	[24]
<i>Nitzschia</i> sp.	52–76	8	17	0	22	–	–	–
<i>Odontella aurita</i> (Lyngbye) C.Agardh, 1832	88	0	0	0	11	[28]	[28]	–
<i>Parlibellus delognei</i> (Van Heurck) E.J. Cox, 1988	54–100	0	0	0	22	[28]	–	[24]
<i>Pleurosigma elongatum</i> W. Smith, 1852	35–75	17	0	0	11	[28]	[28]	[24]
<i>Rhabdonema adriaticum</i> Kützing, 1844	75	8	0	0	0	[28]	–	–
<i>Rhopalodia musculus</i> (Kützing) O.F. Müller, 1899	92	0	0	11	0	[28]	[28]	[21]
<i>Suirella striatula</i> Turpin, 1828	88	0	0	0	11	[28]	–	[21]
<i>Tabularia tabulata</i> (Agardh) Snoeijjs, 1992	66–86	83	100	0	22	[28]	[28]	[21]
<i>Toxarium undulatum</i> J.W. Bailey, 1854	92	0	0	11	0	[28]	–	[21]
<i>Tryblionella apiculata</i> Gregory, 1857	52	8	0	0	0	–	[28]	[21]
Total Diatoms	–	21	10	10	25	22	12	26
Haptophyta								
<i>Calcidiscus leptoporus</i> (G.Murray and V.H.Blackman) Loeblich Jr. and Tappan, 1978	70	0	0	0	11	–	–	[24]
<i>Oolithotus fragilis</i> (Lohmann) Martini and C.Müller, 1972	52	8	17	0	–	–	–	–

Table 2. Cont.

Species	Salinity Range for a Species, Psu	Frequency of Occurrence, %				Found Before		
		May and June 2018		November 2018	June 2019	The Sea of Azov	Eastern Sivash Before 2014	Crimean Hypersaline Lakes
		Bottom	Mat	Bottom	Bottom			
Miozoa								
<i>Prorocentrum balticum</i> (Lohmann) Loeblich III, 1970	69–84	17	0	11	0	–	–	[24]
Cyanobacteria								
<i>Oscillatoria limosa</i> C. Agardh ex Gomont, 1892	54	–	–	0	11	–	–	[11]
<i>Oscillatoria tenuis</i> C. Agardh ex Gomont, 1892	38–70	–	–	11	11	–	–	–
Total number of species	–	23	11	13	29	22	12	27

Pairwise comparison of the lists of species in the three studied periods (May–June 2018, November 2018, and June 2019) using the calculated similarity indices of Jaccard and Czekanowski–Sørensen–Dice (Table 3) showed that the species composition significantly differed in different periods, because in all cases, the values of the similarity coefficients were below critical.

Table 3. Similarity indices between species composition in the different periods (Bay Sivash, 2018–2019).

Index	Compared Pairs			
	Critical Value	May–June 2018 vs. June 2019	May–June 2018 vs. November 2018	November 2018 vs. June 2019
Jaccard	0.42	0.32	0.15	0.29
Czekanowski–Sørensen–Dice	0.59	0.48	0.26	0.45

According to the Student’s t-test, there were no differences in microalgal abundance and biomass at the bottom between May and June of 2018 samples, and they were noted together later (Table 4). Differences in abundance and biomass between May–June of 2018, November 2018, and June 2019 samples were significant ($p = 0.05–0.0001$). In the benthic community, the minimal abundance and biomass were recorded in May 2018, and the maximal abundance and biomass in November 2018. In November of 2018, abundance was 171 and 12 times higher than in June of 2018 and June of 2019, respectively. Spatial variability (according to CV) was different in the different periods: the highest value was in June of 2019 and the lowest in May–June of 2018 (Table 4). At the same time, in May 2018, the microalgae abundance in the mat was two times higher than at the bottom. Cyanobacteria dominated only in one sample in November 2018 (station 14, Table 1), the same was observed in June 2019 (station 13, Table 1).

Table 4. Quantitative characteristics of microphytobenthos in Bay Sivash (2018–2019).

Characteristics		May 2018		June 2018	November 2018	June 2019
		Bottom	Mat	Bottom	Bottom	Bottom
Abundance, cells $\times 10^5 \text{ cm}^{-2}$	Average	0.67	1.30	0.6	111.1	8.95
	min	0.45	0.07	0.05	0.8	0.02
	max	0.80	6.59	0.84	405.3	99.84
	CV	0.286	2.000	0.642	1.405	2.025
Biomass, mg cm^{-2}	Average	0.06	0.143	0.13	6.57	0.26
	min	0.009	0.038	0.01	0.002	0.004
	max	0.14	0.400	0.20	39.25	0.96
	CV	1.286	0.973	0.651	2.070	1.133
Average cell mass in a sample, μg	Average	7.5×10^{-7}	5.2×10^{-6}	2.3×10^{-6}	1.5×10^{-7}	5.03×10^{-5}
	min	2.0×10^{-7}	6.1×10^{-7}	1.8×10^{-6}	2.2×10^{-9}	7.3×10^{-8}
	max	1.7×10^{-6}	1.3×10^{-5}	3.1×10^{-6}	5.3×10^{-7}	3.3×10^{-4}
	CV	1.276	0.844	0.231	1.406	2.195

In all other cases, diatoms dominated (Table 5). The composition of the dominant species is also distinguished in different periods (Table 5). In May–June 2018, four diatom species (*Navicula* sp. 1, *Tabularia tabulata*, *Halamphora coffeiformis*, and *Grammatophora marina*) dominated in different bottom samples, while only two species (*T. tabulata* and *Achnanthes adnate*) were dominant in floating mats. In terms of the contribution of various species to the total number of microalgae, the bottom community and the floating mat differed significantly (Table 5). In November 2018, nine species dominated in different samples, and in June 2019 there were eight such species (Table 5). Only one species, *H. coffeiformis*, was among the dominants in the bottom community during all three studied periods, and only one species, *T. tabulate*, was in two different periods. *A. adnata* was the most dominant species in the floating mat in May and the most common species in the bottom community in November 2018.

Table 5. The contribution of the different species in total microalgae abundance and their frequency of dominance in Bay Sivash (2018–2019).

Species	Average Contribution, %	Minimal Contribution, %	Maximal Contribution, %	CV of Contribution	How Many Times Dominated
May–June 2018, Bottom					
<i>Achnanthes adnata</i>	9	0	28	1.300	0
<i>Cocconeis kujalnitzkensis</i>	8	0	23	1.265	0
<i>Grammatophora marina</i>	13	0	80	2.449	1
<i>Halamphora coffeiformis</i>	18	0	86	1.937	1
<i>Mastogloia braunii</i>	2	0	11	2.449	0
<i>Navicula menisculus</i>	6	0	21	1.590	0
<i>Navicula</i> sp.1	27	0	62	0.767	3
<i>Prorocentrum balticum</i>	3	0	12	1.728	0
<i>Tabularia tabulata</i>	12	0	42	1.210	1

Table 5. Cont.

Species	Average Contribution, %	Minimal Contribution, %	Maximal Contribution, %	CV of Contribution	How Many Times Dominated
May–June 2018, Floating Green Algae Mat					
<i>Achnanthes adnata</i>	20	4	50	0.919	1
<i>Cocconeis kujalnitzkensis</i>	18	4	33	0.639	0
<i>Halamphora coffeiformis</i>	5	0	7	1.425	0
<i>Navicula</i> sp.1	6	1	16	0.928	0
<i>Tabularia tabulata</i>	58	30	83	0.402	5
November 2018, Bottom					
<i>Achnanthes adnata</i>	34	0	100	1.244	3
<i>Amphitetras antediluviana</i>	2	0	20	2.980	0
<i>Ardessonia crystallina</i>	4	0	33	3.000	1
<i>Campylodiscus neofastuosus</i>	11	0	100	3.000	1
<i>Cocconeis kujalnitzkensis</i>	16	0	60	1.477	1
<i>Halamphora coffeiformis</i>	5	0	41	3.000	1
<i>Mastogloia braunii</i>	6	0	56	3.000	1
<i>Oscillatoria tenuis</i>	11	0	98	3.000	1
<i>Prorocentrum balticum</i>	9	0	79	3.000	1
<i>Rhopalodia musculus</i>	4	0	33	3.000	1
<i>Toxarium undulatum</i>	2	0	17	3.000	0
June 2019, Bottom					
<i>Achnanthes adnata</i>	4	0	14	1.453	0
<i>Amphitetras antediluviana</i>	9	0	79	3.000	1
<i>Cocconeis kujalnitzkensis</i>	12	0	27	0.907	0
<i>Cocconeis placentula</i>	11	0	90	2.821	1
<i>Cocconeis scutellum</i>	10	0	65	2.106	1
<i>Grammatophora marina</i>	1	0	10	2.435	0
<i>Gyrosigma balticum</i>	6	0	50	3.000	1
<i>Halamphora coffeiformis</i>	17	0	67	1.658	2
<i>Mastogloia braunii</i>	2	0	14	3.000	0
<i>Navicula menisculus</i>	3	0	30	3.000	0
<i>Navicula</i> sp.	4	0	29	2.476	0
<i>Nitzschia sigma</i>	5	0	43	3.000	1
<i>Nitzschia tenuirostris</i>	1	0	10	2.859	0
<i>Nitzschia</i> sp.	3	0	14	2.016	0
<i>Oscillatoria limosa</i>	5	0	48	3.000	1
<i>Parlibellus delognei</i>	1	0	10	2.537	0
<i>Pleurosigma elongatum</i>	3	0	25	3.000	0
<i>Surirella fastuosa</i>	1	0	13	3.000	0
<i>Tabularia tabulata</i>	4	0	34	2.722	1

For all periods, there was a general trend of an increase of the bottom microalgae abundance with salinity, but it was insignificant.

In November 2018, a positive reliable correlation was found between the total number of microalgae and the number of species ($R = 0.797$, $p = 0.005$) (Figure 2); however, in other periods such a reliable unambiguous relationship was not noted.

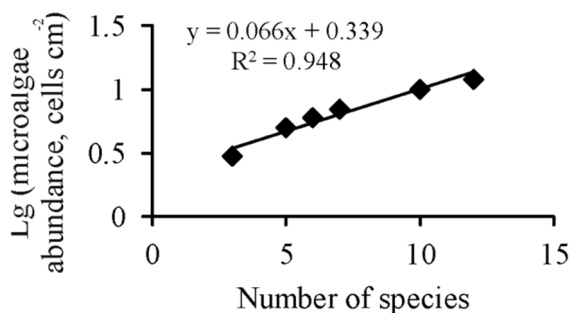


Figure 2. Dependence of the benthic microalgae abundance on the abundance of their species (Sivash Bay, June 2019).

In May–June 2018 and June 2019, no correlations were observed between the abundance/biomass of benthic microalgae with salinity, the concentrations of TSS, and DOM. In November 2018, a significant positive correlation was noted between the concentration of TSS and the total biomass of algae ($R = 0.985$, $p = 0.0005$):

$$B = 0.584 \text{ TSS} - 2.992 \quad (10)$$

where B is the biomass, mg cm^{-2} , and TSS is the concentration of suspended matter, mg L^{-1} .

According to the calculated CV values, the degree of spatial heterogeneity of abundance and biomass was minimal in May–June 2018, and maximal in June 2019 (Table 4). In May, the average cell mass was significantly greater in the mat than on the bottom ($p = 0.05$), on average by 5.3 times (Table 4).

In the bottom community, the average cell mass significantly changed over time (Table 4), the maximal was in November 2018 (average $15.0 \times 10^{-2} \mu\text{g}$), and the minimal in May 2018 ($7.5 \times 10^{-4} \mu\text{g}$). The average cell size of *A. adnata* (average length $61 \mu\text{m}$) was significantly ($p = 0.05$), at 1.6 times, larger in November 2018 than in the spring–summer months (average length $38.2 \mu\text{m}$) (Table 6). For all other species, no significant temporal changes in cell size were observed (Table 6). In May–June 2018, a significant negative relationship between the cell length of *A. adnata* and salinity ($R = -0.788$, $p = 0.005$) and DOM concentration ($R = -0.807$, $p = 0.005$) was noted, which can be approximated by the following equations:

$$L = 262.4 - 48.5 \text{ Ln}(S) \quad (11)$$

and

$$L = 119.6 - 16.6 \text{ DOM} \quad (12)$$

where L is the average cell length, μm , S is salinity, psu , and DOM is the concentration of DOM , mg L^{-1} .

For other species, some correlations were not found. In November 2018, no correlations between the cell size and the measured environmental factors were revealed. In June 2019, the cell size of *Cocconeis scutellum* was significantly negatively correlated with salinity ($R = -0.963$, $p = 0.02$) and DOM ($R = -0.901$, $p = 0.05$):

$$l = 27.7 - 0.7 s \quad (13)$$

and

$$L = 27.7 - 1.6 \text{ DOM} \quad (14)$$

At the same time, an opposite pattern was noted for *Cocconeis kujalnitzkensis*, a linear positive correlation with salinity ($R = 0.812$, $p = 0.025$) and with DOM concentration ($R = 0.744$, $p = 0.03$):

$$L = 0.2 S - 1.2 \quad (15)$$

and

$$L = 9.01 + 4.8 \text{ DOM} \quad (16)$$

For other species, the influence of these factors on the size was not revealed.

Table 6. Averages sizes of different microalgae species (Bay Sivash, 2018–2019).

Species	Cell Sizes							
	May–June 2018				November 2018		June 2019	
	Bottom		Mat		Bottom		Bottom	
	L, μm	H, μm	L, μm	H, μm	L, μm	H, μm	L, μm	H, μm
Ochrophyta								
<i>Achnanthes adnata</i>	52.5	17.5	57.9	23.3	61.1	18.0	42.0	20.3
<i>Amphitetras antediluviana</i>	–	–	–	–	94.0	76.0	81.0	75.0
<i>Amphora macilenta</i> var. <i>maeotica</i>	–	–	–	–	34.0	13.0	–	–
<i>Amphora ovalis</i>	–	–	–	–	–	–	31.0	13.0
<i>Amphora</i> sp.	–	–	35.0	15.0	–	–	–	–
<i>Ardissonea crystallina</i>	–	–	–	–	76.0	6.0	67.0	7.0
<i>Campylodiscus neofastuosus</i>	–	–	–	–	93.0	76.0	97.0	83.0
<i>Cocconeis kujalnitzkensis</i>	13.8	10.6	16.8	12.1	14.3	8.3	12.8	6.7
<i>Cocconeis scutellum</i>	–	–	–	–	–	–	21.0	13.5
<i>Cocconeis placentula</i>	–	–	–	–	–	–	22.8	14.0
<i>Grammatophora marina</i>	62.5	15.0	–	–	–	–	33.0	14.5
<i>Gyrosigma balticum</i>	–	–	–	–	–	–	342.0	32.0
<i>Halamphora coffeiformis</i>	31.7	12.5	22.5	10.6	24.0	13.0	25.9	13.0
<i>Mastogloia braunii</i>	30.0	7.5	–	–	41.0	14.0	–	–
<i>Navicula menisculus</i>	20.0	5.0	25.0	4.4	–	–	18.0	3.0
<i>Navicula</i> sp. 1	11.8	2.7	12.5	2.7	–	–	12.0	3.0
<i>Navicula</i> sp. 2	10.0	2.5	–	–	–	–	–	–
<i>Nitzschia hybrida</i> var. <i>hyalina</i>	25.0	5.0	20.0	5.0	–	–	36.0	13.0
<i>Nitzschia sigma</i>	–	–	–	–	–	–	72.0	3.0
<i>Nitzschia tenuirostris</i>	29.5	2.5	22.5	2.0	–	–	20.5	3.0
<i>Nitzschia</i> sp.	50.0	2.5	–	–	–	–	52.0	3.5
<i>Odontella aurita</i>	–	–	–	–	–	–	56.0	40.0
<i>Parlibellus delognei</i>	–	–	–	–	–	–	26.5	6.0
<i>Pleurosigma elongatum</i>	–	–	–	–	–	–	319.0	34.0
<i>Rhopalodia musculus</i>	–	–	–	–	34.0	31.0	–	–
<i>Surirella fastuosa</i>	–	–	–	–	106.0	84.0	–	–
<i>Tabularia tabulata</i>	50.3	4.0	55.0	4.1	–	–	59.0	5.5
<i>Toxarium undulatum</i>	–	–	–	–	583.0	67.0	–	–

Table 6. Cont.

Species	Cell Sizes							
	May–June 2018				November 2018		June 2019	
	Bottom		Mat		Bottom		Bottom	
	L, μm	H, μm	L, μm	H, μm	L, μm	H, μm	L, μm	H, μm
Haptophyta								
<i>Oolithotus fragilis</i>	15.0	15.0	–	–	–	–	–	–
Miozoa								
<i>Prorocentrum balticum</i>	12.5	8.8	–	–	15.0	13.0	–	–
Cyanobacteria								
<i>Oscillatoria limosa</i>	–	–	–	–	–	–	22.5	4.5
<i>Oscillatoria tenuis</i>	–	–	–	–	11.0	5.0	–	–

L—cell length; H—cell width.

4. Discussion

A total of 27 species of microalgae were found in hypersaline lakes of Crimea previously (Table 2) [11,21,24]. The calculated similarity coefficients of Jaccard (32%) and Chekanovsky (51%) between species composition in the Crimean hypersaline lakes and that currently found in Bay Sivash turned out to be lower than their critical values. Therefore, it can be concluded that the modern complex of bottom microalgae in Sivash significantly differs from that of the Crimean hypersaline lakes. Of all diatom species found in the Sivash, 71% were also noted in the Sea of Azov (Table 2), while the total number of diatom species in the Sea of Azov is 1085 [28]. The calculated Jaccard's and Chekanovsky's indexes gave very small values of similarity, likely due to the number of species found in Sivash being much less than that found in the sea, at 1.5 orders of magnitude. Therefore, one can confidently assert that the species composition in the bay was primarily formed by the Azov–Black Sea species. Before the onset of the salinity increase, 61 species of microalgae were found in Eastern Sivash [28,36], of which only 12 have now been recorded, 31% of the current species richness. In the structure of the microphytobenthos in Eastern Sivash, after a sharp increase in salinity, substantial changes in the microalgal species richness and composition have occurred. The total number of identified species is currently 39, i.e., species richness decreased by 36% after the closure of the canal. A comparison of the lists of species before and after the closure of the canal indicated a significant change in the microphytobenthos species composition. Currently, the most common dominant species are *A. adnata*, inhabiting both the hypersaline lakes of the Crimea and the Sea of Azov, as well as *C. kujalnitzkensis*, only recorded in the hypersaline lakes of Crimea and lagoons of the Northwestern Black Sea (Table 2). Cyanobacteria (more than 100 species) are common components of the microphytobenthos of hypersaline water bodies of Crimea, including those found in Bay Sivash [11,37]. *Calcidiscus leptoporus* (Haptophyta) and *Prorocentrum balticum* (Miozoa) were previously found in the hypersaline lakes of Crimea [24], and in the Black Sea [38].

Several common diatom species in hypersaline waters have a very wide geographic distribution, which indicates the presence of mechanisms for their long-distance transport (winds or birds). For example, *H. coffeiformis*, *Cocconeis placentula*, *Amphora ovalis*, *Mastogloia braunii*, *Nitzschia hybrida*, *Campylodiscus neofastuosus*, and *Tryblionella apiculata*, are common species in the marine and continental hypersaline waters not only in Europe but also in Asia [22,39], North and South America [17–20,40], Australia [41,42], and Africa [43,44]. At the same time, *C. kujalnitzkensis* was previously found, in addition to Crimea, only in hypersaline lagoons of the northwestern part of the Black Sea [45]. Consequently, both narrow/local Azov–Black Sea endemics and cosmopolitans are represented in the composition of common species. The composition of species in the *Cladophora* mats and at

the bottom did not differ, but the number of species in the mats is lower, perhaps due to the mats' shorter life, their destruction every year in the autumn–winter period and during rare strong storms in summer.

In our case, 15 species were recorded at salinities of 80–90 psu, and 10 species at higher salinities, which contribute 64% of all species found in our study. While it should be noted that 55% of all species were found singularly, some of them may be also highly halotolerant. Numerous studies showed that salinity in the range of 50–150 psu is not the main factor limiting the distribution of a sufficiently large number of benthic microalgae species [46–49]. One of the main mechanisms that allows algae to exist in a hypersaline environment is the release of a significant amount of exosaccharides (EPS) into the environment with the creation of an EPS matrix, in which cells live [50,51].

The noted quantitative development of benthic microalgae was quite high (Table 3), which was previously noted in other hypersaline water bodies of Crimea [21,24] and other regions [15,52]. Moreover, in May 2018, microalgae had a higher average abundance in the mats than on the bottom. The intensive development of microalgae on the *Cladophora* filaments is a well-known phenomenon and has been shown in different types of water bodies [24]. The highest values of microalgal abundance and biomass in November can be explained by the growth of the microphytobenthos from spring to autumn. The strong autumn–winter storms lead to the destruction of the microphytobenthos, as well as floating mats in the shallow bay, and total abundance, and as a result, the biomass of microalgae drops on the bottom. It should be noted that in June 2019, microalgal abundance and biomass were significantly higher than in May–June 2018, as was the average cell size (Table 3). Probably, to a certain extent, this is due to an increase in salinity during this period: the average salinity in May 2018 was 64 psu (CV = 0.292), in November 2018 it was 74 psu (CV = 0.292), and in June 2019 it was 73 psu. This assumption is consistent with the fact that, in the spatial distribution, the microalgae abundance also may positively correlate with salinity. The dependence of the microalgae abundance on the salinity growth can be partially explained by the fact that with the salinity increase, the number of animals capable of consuming microalgae decreases in the bay [25,26]. A positive relationship between the abundance of bottom microalgae and salinity was also noted for water bodies in other regions [15,48], in particular for Mediterranean lagoons [52,53].

However, it is unlikely that only the salinity increase caused an increase in the number of bottom microalgae in the lagoon. Many characteristics have changed in the bay, for example, the concentration of total suspended matter and dissolved organic matter has increased. The temperature regime and oxygen concentration have also changed in the lagoon, as shown before [27,29]. Some drops of oxygen content occurred due to a decreasing oxygen solubility with a salinity increase, and some increase of temperature may be explained by a decrease of the specific heat capacity of water due to a salinity growth. The significant changes in other biotic components (zooplankton and zoobenthos), including in the macrophyte community, were also recorded here before [27,29]. Powerful thickets of marine grass *Zostera*, on which epiphyton was massively developed, have disappeared [28], and mats of green filamentous algae *Cladophora* began to develop intensively [29].

It can be assumed that a sharp increase in salinity destabilized the benthic microalgal community, like other communities in the bay [25–27,29], with a decrease in their species richness and abundance. It is known that usually there is an increase in species diversity, average size, and total number of species in communities during restoration after ecological disasters [54–56]. It can be assumed that the species composition and indicators of quantitative development will stabilize soon after the cessation of salinity growth in the lagoon. Likely the frequent anoxia/hypoxia events occurring now in Sivash do not greatly inhibit this transition to the new stable state because experiments have shown that the microphytobenthos can recover from such events rather quickly [6].

5. Conclusions

Summarizing all the above, the authors can make a general conclusion that salinity in the range from 30 to 150 psu is not the only or main factor that determines the species composition of the microphytobenthos. Other factors (the concentration of total suspended matter, etc.) can play an equally important role. At the same time, quantitative indicators of microphytobenthos development may positively correlate with salinity. This study of the microphytobenthos in Bay Sivash during the period of its salinization is the first, and therefore, it does not provide answers to many interesting questions. The continuation of such studies will make it possible to understand more about the regularities of microphytobenthos transformation during the period of sharp changes in the environment.

Author Contributions: Conceptualization, N.S.; methodology, N.S., D.B. and E.A.; field investigation and sampling, N.S. and E.A.; microalgae sample processing and microalgae species identification, D.B.; data formal analysis, N.S. and E.A.; writing—original draft and final text, N.S.; first draft writing—review and editing, N.S., D.B. and E.A. All authors have read and agreed to the published version of the manuscript.

Funding: Sample processing, data analysis, and this manuscript writing was supported by the Russian Science Foundation grant number 18-16-00001; the part concerning the long-term study of the Bay Sivash environment was conducted in the framework by the state assignment of A.O. Kovalevsky Institute of Biology of the Southern Seas of RAS number 121041500203-3.

Institutional Review Board Statement: Not applicable.

Informed Consent Statement: Not applicable.

Data Availability Statement: All data used in this study are available upon request from the corresponding author.

Acknowledgments: The authors are grateful to Alexander Latushkin for his help conducting a field study and obtaining data on TSS and DOM as well as Bindy Datson for her selfless work in improving the English of the manuscript.

Conflicts of Interest: The authors declare no conflict of interest.

References

1. Brito, A.; Newton, A.; Tett, P.; Fernandes, T.F. Temporal and spatial variability of microphytobenthos in a shallow lagoon: Ria Formosa (Portugal). *Estuar. Coast. Shelf Sci.* **2009**, *83*, 67–76. [[CrossRef](#)]
2. Lake, S.J.; Brush, M.J. The contribution of microphytobenthos to total productivity in upper Narragansett Bay, Rhode Island. *Estuar. Coast. Shelf Sci.* **2011**, *95*, 289–297. [[CrossRef](#)]
3. Belando, M.D.; Marin, A.; Aboal, M. *Licmophora* species from a Mediterranean hypersaline coastal lagoon (Mar Menor, Murcia, SE Spain). *Nova Hedwig.* **2012**, *141*, 275–288.
4. Andersen, T.J.; Lund-Hansen, L.C.; Pejrup, M.; Jensen, K.T.; Mouritsen, K.N. Biologically induced differences in erodibility and aggregation of subtidal and intertidal sediments: A possible cause for seasonal changes in sediment deposition. *J. Mar. Syst.* **2005**, *55*, 123–138. [[CrossRef](#)]
5. Kanaya, G.; Takagi, S.; Kikuchi, E. Dietary contribution of the microphytobenthos to infaunal deposit feeders in an estuarine mudflat in Japan. *Mar. Biol.* **2008**, *155*, 543–553. [[CrossRef](#)]
6. Larson, F.; Sundbäck, K. Role of microphytobenthos in recovery of functions in a shallow-water sediment system after hypoxic events. *Mar. Ecol. Prog. Ser.* **2008**, *357*, 1–6. [[CrossRef](#)]
7. Brito, A.C.; Fernandes, T.F.; Newton, A.; Facca, C.; Tett, P. Does microphytobenthos resuspension influence phytoplankton in shallow systems? A comparison through a Fourier series analysis. *Estuar. Coast. Shelf Sci.* **2012**, *110*, 77–84. [[CrossRef](#)]
8. Dunn, R.J.; Welsh, D.T.; Jordan, M.A.; Waltham, N.J.; Lemckert, C.J.; Teasdale, P.R. Benthic metabolism and nitrogen dynamics in a sub-tropical coastal lagoon: Microphytobenthos stimulate nitrification and nitrate reduction through photosynthetic oxygen evolution. *Estuar. Coast. Shelf Sci.* **2012**, *113*, 272–282. [[CrossRef](#)]
9. Schreiber, R.A.; Pennock, J.R. The relative contribution of benthic microalgae to total microalgal production in a shallow sub-tidal estuarine environment. *Ophelia* **1995**, *42*, 335–352. [[CrossRef](#)]
10. Shadrin, N.V. Is it possible to quantitatively assess the role of algobacterial films in a water body? In *Fossil and Recent Biofilms: A Natural History of Life on Earth*; Krumbein, W.E., Paterson, D.M., Zavarzin, G.A., Eds.; Springer: Dordrecht, The Netherlands, 2003; pp. 353–361.

11. Shadrin, N.V.; Mikhodyuk, O.S.; Naidanova, O.G.; Voloshko, L.N.; Gerasimenko, L.M. Bottom cyanobacteria of the hypersaline lakes of Crimea. In *Microalgae of the Black Sea: Problems of Biodiversity Preservation and Biotechnological Use*; Tokarev, Y.N., Finenko, Z.Z., Shadrin, N.V., Eds.; EKOSI-Gidrophyzika: Sevastopol, Ukraine, 2008; pp. 100–112. (In Russian)
12. Senicheva, M.I.; Gubelit, Y.I.; Prazukin, A.V.; Shadrin, N.V. Phytoplankton of hypersaline lakes of Crimea. In *Microalgae of the Black Sea: Problems of Biodiversity Preservation and Biotechnological Use*; Tokarev, Y.N., Finenko, Z.Z., Shadrin, N.V., Eds.; EKOSI-Gidrophyzika: Sevastopol, Ukraine, 2008; pp. 93–99. (In Russian)
13. Lukatelich, R.J.; McComb, A.J. Distribution and abundance of benthic microalgae in a shallow southwestern Australian estuarine system. *Mar. Ecol. Prog. Ser.* **1986**, *27*, 287–297. [[CrossRef](#)]
14. Segal, R.D.; Waite, A.M.; Hamilton, D.P. Transition from planktonic to benthic algal dominance along a salinity gradient. *Hydrobiologia* **2006**, *556*, 119–135. [[CrossRef](#)]
15. Asencio, A.D. Permanent salt evaporation ponds in a semi-arid Mediterranean region as model systems to study primary production processes under hypersaline conditions. *Estuar. Coast. Shelf Sci.* **2013**, *124*, 24–33. [[CrossRef](#)]
16. Shadrin, N.; Anufriieva, E. Ecosystems of hypersaline waters: Structure and trophic relations. *Zhurnal Obs. Biol.* **2018**, *79*, 418–427. (In Russian)
17. Siqueiros-Beltrones, D.A. Association structure of benthic diatoms in a hypersaline environment. *Cienc. Mar.* **1990**, *16*, 101–127. [[CrossRef](#)]
18. Kociolek, J.P.; Herbst, D.B. Taxonomy and distribution of benthic diatoms from Mono Lake, California, U.S.A. *Trans. Am. Microsc. Soc.* **1992**, *111*, 338–355. [[CrossRef](#)]
19. Wilson, S.E.; Cumming, B.F.; Smol, J.P. Diatom-salinity relationships in 111 lakes from the Interior Plateau of British Columbia, Canada: The development of diatom-based models for paleosalinity reconstructions. *J. Paleolimnol.* **1994**, *12*, 197–221. [[CrossRef](#)]
20. Sylvestre, F.; Beck-Eichler, B.; Duleba, W.; Debenay, J.P. Modern benthic diatom distribution in a hypersaline coastal lagoon: The Lagoa de Araruama (RJ), Brazil. *Hydrobiologia* **2001**, *443*, 213–231. [[CrossRef](#)]
21. Nevrova, E.L.; Shadrin, N.V. Benthic diatoms in Crimean saline lakes. *Mar. Ecol. J.* **2005**, *4*, 61–71. (In Russian)
22. Sapozhnikov, F.V.; Ivanishcheva, P.S.; Simakova, U.V. Modern assemblage changes of benthic algae as a result of hypersalinization of the Aral Sea. *J. Mar. Syst.* **2009**, *76*, 343–358. [[CrossRef](#)]
23. Schagerl, M. *Soda Lakes of East Africa*; Springer Nature: Cham, Switzerland, 2016; p. 408.
24. Prazukin, A.; Shadrin, N.; Balycheva, D.; Firsov, Y.; Lee, R.; Anufriieva, E. *Cladophora* spp. (Chlorophyta) modulate environment and create a habitat for microalgae in hypersaline waters. *Eur. J. Phycol.* **2020**. [[CrossRef](#)]
25. Shadrin, N.; Kolesnikova, E.; Revkova, T.; Latushkin, A.; Dyakov, C.; Anufriieva, E. Macrostructure of benthos along a salinity gradient: The case of Sivash Bay (the Sea of Azov), the largest hypersaline lagoon worldwide. *J. Sea Res.* **2019**, *154*, 101811. [[CrossRef](#)]
26. Shadrin, N.; Kolesnikova, E.; Revkova, T.; Latushkin, A.; Chepyzhenko, A.; Drapun, I.; Dyakov, N.; Anufriieva, E. Do separated taxa react differently to a long-term salinity increase? The meiobenthos changes in Bay Sivash, largest hypersaline lagoon worldwide. *Knowl. Manag. Aquat. Ecosyst.* **2019**, *420*, 36. [[CrossRef](#)]
27. Anufriieva, E.; Shadrin, N. The long-term changes in plankton composition: Is Bay Sivash transforming back into one of the world's largest habitats of *Artemia* sp. (Crustacea, Anostraca)? *Aquac. Res.* **2020**, *51*, 341–350. [[CrossRef](#)]
28. Bondarenko, A.V. Microalgae of the benthos of the Crimean coastal waters in the Sea of Azov. PhD Thesis, A.O. Kovalevsky Institute of Biology of the South Seas of RAS, Sevastopol, Russia, 2017; 176p. (In Russian)
29. Shadrin, N.V.; Anufriieva, E.V.; Kipriyanova, L.M.; Kolesnikova, E.A.; Latushkin, A.A.; Romanov, R.E.; Sergeeva, N.G. The political decision caused the drastic ecosystem shift of the Sivash Bay (the Sea of Azov). *Quat. Int.* **2018**, *475*, 4–10. [[CrossRef](#)]
30. Guiry, M.D.; Guiry, G.M. AlgaeBase. World-wide electronic publication, National University of Ireland, Galway, Ireland. 2020. Available online: <http://www.algaebase.org> (accessed on 13 May 2020).
31. Oksiyuk, O.P.; Yurchenko, V.V. About the weight of diatoms. *Hydrobiol. J.* **1971**, *7*, 116–119. (In Russian)
32. Bryantseva, J.V.; Lyakh, A.M.; Sergeeva, A.V. *Calculation of Volumes and Surface Areas of the Black Sea Unicellular Algae*; Publishing House of the Institute of Biology of the South Seas: Sevastopol, Ukraine, 2005; p. 25. (In Russian)
33. Müller, P.H.; Neuman, P.; Storm, R. *Tafeln der Mathematischen Statistik*; VEB Fachbuchverlag: Leipzig, Germany, 1979; p. 272.
34. Thode, H.C. *Testing for Normality*; Marcel Dekker Inc.: New York, NY, USA, 2002; 271p.
35. Semkin, B.I. On the relation between mean values of two measures of inclusion and measures of similarity. *Bull. Bot. Gard. Inst. Far East. Branch Ras* **2009**, *3*, 91–101. (In Russian)
36. Barinova, S.; Bondarenko, A.; Ryabushko, L.; Kapranov, S. Microphytobenthos as an indicator of water quality and organic pollution in the western coastal zone of the Sea of Azov. *Oceanol. Hydrobiol. Stud.* **2019**, *48*, 125–139. [[CrossRef](#)]
37. Anufriieva, E.V.; Shadrin, N.V.; Shadrina, S.N. History of research on biodiversity in Crimean hypersaline waters. *Arid Ecosyst.* **2017**, *7*, 52–58. [[CrossRef](#)]
38. Ryabushko, L.I. *Microphytobenthos of the Black Sea*; ECOSI-Gidrophyzika: Sevastopol, Russia, 2013; 416p. (In Russian)
39. Sapozhnikov, P.V.; Kalinina, O.Y. Main Results of Observations of Changes in Bottom Biota and Ichthyofauna of the Large Aral Sea in the Period 2002–2017. *Hydrosphere Ecol.* **2018**, *1*. Available online: <http://hydrosphere-ecology.ru/109> (accessed on 30 May 2021). (In Russian)
40. Siqueiros-Beltrones, D.A.; Morzaria-Luna, H. New records of marine benthic diatom species for the Northwestern Mexican region. *Oceanides* **1999**, *14*, 89–95.

41. Blinn, D.; Halse, S.; Pinder, A.; Shiel, R. Diatom and micro-invertebrate communities and environmental determinants in the western Australian wheatbelt: A response to salinization. *Hydrobiologia* **2004**, *528*, 229–248. [[CrossRef](#)]
42. Taukulis, F.E.; John, J. Development of a diatom-based transfer function for lakes and streams severely impacted by secondary salinity in the south-west region of Western Australia. *Hydrobiologia* **2009**, *626*, 129–143. [[CrossRef](#)]
43. Gasse, F.; Juggins, S.; Khelifa, L.B. Diatom-based transfer functions for inferring past hydrochemical characteristics of African lakes. *Palaeogeogr. Palaeoclimatol. Palaeoecol.* **1995**, *117*, 31–54. [[CrossRef](#)]
44. Bate, G.; Smailes, P. The response of the diatom flora of St Lucia Lake and estuary, South Africa, to a severe drought. *Afr. J. Aquat. Sci.* **2008**, *33*, 1–15. [[CrossRef](#)]
45. Gerasimiuk, V.P. Microalgae of the north-western Black Sea coast estuaries. *Int. J. Algae* **2018**, *20*, 109–120. [[CrossRef](#)]
46. Dor, I.; Ehrlich, A. The effect of salinity and temperature gradients on the distribution of littoral microalgae in experimental solar ponds, Dead Sea area, Israel. *Mar. Ecol.* **1987**, *8*, 193–205. [[CrossRef](#)]
47. Clavero, E.; Hernández-Mariné, M.; Grimalt, J.O.; Garcia-Pichel, F. Salinity tolerance of diatoms from thalassic hypersaline environments. *J. Phycol.* **2000**, *36*, 1021–1034. [[CrossRef](#)]
48. Dolapsakis, N.P.; Tafas, T.; Abatzopoulos, T.J.; Ziller, S.; Economou-Amilli, A. Abundance and growth response of microalgae at Megalon Embolon solar saltworks in northern Greece: An aquaculture prospect. *J. Appl. Phycol.* **2005**, *17*, 39–49. [[CrossRef](#)]
49. Häusler, S.; Weber, M.; de Beer, D.; Ionescu, D. Spatial distribution of diatom and cyanobacterial mats in the Dead Sea is determined by response to rapid salinity fluctuations. *Extremophiles* **2014**, *18*, 1085–1094. [[CrossRef](#)] [[PubMed](#)]
50. Abdullahi, A.S.; Underwood, G.J.; Gretz, M.R. Extracellular matrix assembly in diatoms (Bacillariophyceae). V. Environmental effects on polysaccharide synthesis in the model diatom, *Phaeodactylum tricornutum*. *J. Phycol.* **2006**, *42*, 363–378. [[CrossRef](#)]
51. Steele, D.J.; Franklin, D.J.; Underwood, G.J. Protection of cells from salinity stress by extracellular polymeric substances in diatom biofilms. *Biofouling* **2014**, *30*, 987–998. [[CrossRef](#)]
52. Abdel-Karim, M.S.; Ali, M.H.; Sayed, M.F. Spatial and temporal distribution of micro benthic algae in hyper saline Mediterranean Lagoon (Bardawil Lagoon, Egypt), multivariate analysis approach. *Egypt. J. Aquat. Res.* **2006**, *32*, 271–291.
53. Blasutto, O.; Cibic, T.; De Vittor, C.; Umani, S.F. Microphytobenthic primary production and sedimentary carbohydrates along salinity gradients in the lagoons of Grado and Marano (Northern Adriatic Sea). *Hydrobiologia* **2005**, *550*, 47–55. [[CrossRef](#)]
54. Christensen, N.L. Succession and natural disturbance: Paradigms, problems, and preservation of natural ecosystems. In *Ecosystem Management for Parks and Wilderness*; Agee, J.K., Johnson, D.R., Eds.; University of Washington Press, Institute of Forest Resources Contribution: Seattle, WA, USA, 1988; No. 65, pp. 62–86.
55. Janousek, C.N.; Currin, C.A.; Levin, L.A. Succession of microphytobenthos in a restored coastal wetland. *Estuaries Coasts* **2007**, *30*, 265–276. [[CrossRef](#)]
56. Pennesi, C.; Danovaro, R. Assessing marine environmental status through microphytobenthos assemblages colonizing the Autonomous Reef Monitoring Structures (ARMS) and their potential in coastal marine restoration. *Mar. Pollut. Bull.* **2017**, *125*, 56–65. [[CrossRef](#)]